Journal of Nuclear Materials 438 (2013) S72–S77

Contents lists available at SciVerse ScienceDirect

Journal of Nuclear Materials

journal homepage: www.elsevier.com/locate/jnucmat

Empiricial scaling of inter-ELM power widths in ASDEX Upgrade and JET

T. Eich [b,*], B. Sieglin [b], A. Scarabosio [b], A. Herrmann [b], A. Kallenbach [b], G.F. Matthews [c], S. Jachmich [d], S. Brezinsek [e], M. Rack [e], R.J. Goldston [f], ASDEX Upgrade Team [b], JET-EFDA contributors [a,b,1]

[a] JET-EFDA, Culham Science Centre, Abingdon OX14 3DB, UK
[b] Max-Planck-Institut für Plasmaphysik, EURATOM Association, Boltzmannstr. 2, D-85748 Garching, Germany
[c] EURATOM/CCFE Association, Culham Science Centre, Abingdon, Oxon OX14 3DB, UK
[d] ERM-KMS, EURATOM Association, Brussels, Belgium
[e] IEK-4, Forschungszentrum Jülich, EURATOM Association, Germany
[f] Princeton Plasma Physics Labaratory, Princeton, NJ 08543, USA

ARTICLE INFO

Article history:
Available online 11 January 2013

ABSTRACT

The SOL power decay length (λ_q) deduced from analysis of fully attached divertor heat load profiles from two tokamaks, JET and ASDEX Upgrade with carbon plasma facing components, are presented. Interpretation of the target heat load profiles is performed by using a 1D-fit function which disentangles the upstream λ_q and an effective diffusion in the divertor (S), the latter essentially acting as a power spreading parameter in the divertor volume. It is shown that the so called integral decay length λ_{int} is approximately given by $\lambda_{int} \approx \lambda_q + 1.64 \times S$. An empirical scaling reveals parametric dependency $\lambda_q/\mathrm{mm} \simeq 0.9 \cdot B_T^{-0.7} q_{cyl}^{1.2} P_{SOL}^{0} R_{geo}^{0}$ for type-I ELMy H-modes. Extrapolation to ITER gives $\lambda_q \simeq 1$ mm. Recent measurements in JET-ILW and from ASDEX Upgrade full-W confirm the results. It is shown that a regression for the divertor power spreading parameter S is not yet possible due to the large effect of different divertor geometries of JET and ASDEX Upgrade Divertor-I and Divertor-IIb.

1. Introduction

In diverted tokamak devices, plasmas are confined in a toroidally symmetric region of closed magnetic field lines referred to as the core plasma. These are surrounded by an open field line region, known as the scrape-of-layer (SOL), with field lines that begin and end on material surfaces of a structure known as a divertor. Energy is temporarily confined within the core plasma, but eventually flows outwards, partially through radiation, but with a significant energy heat flux (q) flowing into the SOL and, through it, to the divertor. This power flow to the divertor must be below that which can be sustained by the divertor surface material and this places an important restriction on the plasmas which are permissible. The integral power decay width, λ_{int}, is effectively the radial width of the region on the divertor target plates onto which power flows. The latter is a critical quantity for determining the divertor peak heat load (q_{max}) for current and future devices. Closely related to this parameter is the power decay length in the SOL, λ_q. The high confinement mode, or H-mode [1], is chosen for the baseline scenario of ITER [32] and is also a candidate for future fusion reactors. The mode is characterised by an edge transport barrier just inside the last closed flux surface which is often subject to periodic relaxations, called edge-localised-modes (ELMs) [2]. This paper is concerned with determining both λ_{int} and λ_q during H-mode plasmas. It reviews and builds on previous work to determine λ_q [9]. Additional ASDEX Upgrade data from the open Divertor-I are presented to support this. In addition, the empirical model of λ_q first presented in [9] is further validated by showing agreement with an ASDEX Upgrade fit and new data from JET and ASDEX Upgrade plasmas with tungsten divertors. A first comparative study of L-mode and H-mode power decay length scalings is also presented.

As for Ref. [9], the work is based on divertor heat load measurements from fast (10 kHz) infrared camera systems installed on both JET and ASDEX Upgrade. Both systems have a spatial resolution of 1.7 mm. As can be seen for the JET plasma in Fig. 1, during ELMs, toroidally asymmetric heat fluxes are observed on the divertor target [3–5] with large power decay lengths [6]. In addition, and also shown in Fig. 1, ELMs are often associated with radial displacements of the strike point on the divertor target, comparable in size to the power decay length [7]. From Fig. 2, it can be seen that a similar behaviour is seen in ASDEX Upgrade only with smaller radial displacements of the strike points, <5 mm [8]. Thus, ELM heat loads appear to be different in nature to the inter-ELM heat loads considered here and must be treated separately. For this reason, inter-ELM periods from 90% to 99% of the ELM cycle period are defined and only data from these are used in the rest of this paper.

* Corresponding author.
E-mail address: teich@ipp.mpg.de (T. Eich).

[1] See the Appendix of F. Romanelli et al., Proceedings of the 23rd IAEA Fusion Energy Conference 2010, Daejeon, Korea.

0022-3115/$ - see front matter © 2013 Euratom. Published by Elsevier B.V. All rights reserved.
http://dx.doi.org/10.1016/j.jnucmat.2013.01.011

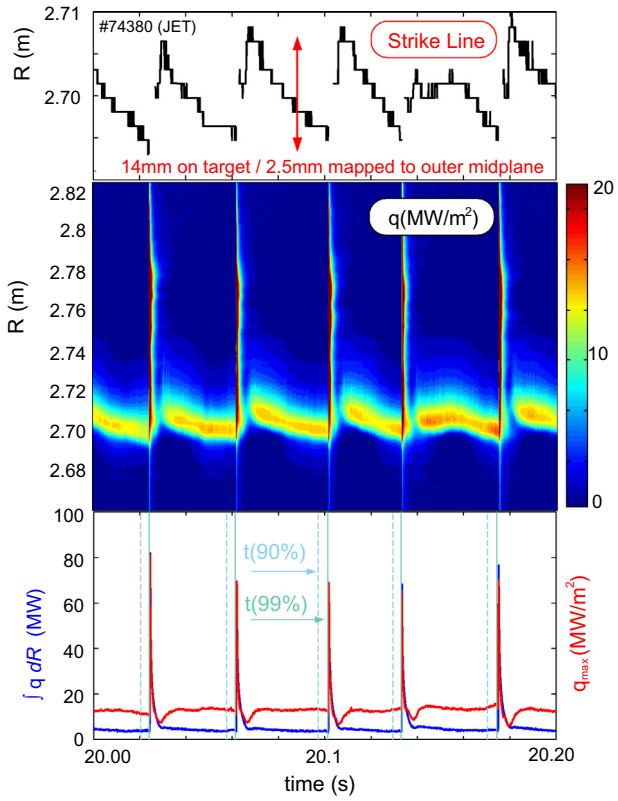

Fig. 1. Evolution of heat flux and the inferred strike line position on the divertor target for a typical JET discharge during type-I ELMy phase.

2. Database of JET and ASDEX Upgrade discharges

Using the diagnosis outlined in Section 1, a database of type-I ELMy H-mode discharges from JET and ASDEX Upgrade has been constructed. The new database extends the previous version [9] which comprised 56 discharges from JET and 11 from ASDEX Upgrade with the Div-IIb divertor. 11 further ASDEX Upgrade Div-IIb discharges have been added as well as 4 discharges with the more open Div-I divertor [10]. This enables the study the influence of the divertor target tiles and magnetic geometry on λ_{int}. In addition, 4 new JET discharges have been added. The range of key parameters in the new database is summarised in Table 1. Here,I_p is the plasma current, B_T the toroidal magnetic field, q_{95} the edge safety factor, P_h the heating power, δ the averaged triangularity, Z_{eff} the effective charge, and f_{GW} the Greenwald density fraction. The aspect ratio of both machines, defined as $\epsilon = a/R_{geo}$, is $\epsilon = 0.32$, where R_{geo} is the major geometrical radius and a the minor radius. The plasma elongation is $\kappa = 1.8$ for both devices. Heat flux profiles are analysed with minimal gas puffing and in the absence of power detachment with carbon divertor plasma-facing components. However, it should be noted that the divertor geometries for JET and ASDEX Upgrade are quite different. JET imposes an open divertor geometry, i.e. the outer strike line is positioned on the outer horizontal target tile [11]. Additionally, for JET, only such discharges can be analysed with IR due to the observation geometry (for details see [6]). ASDEX Upgrade Div-IIb runs regularly with both strike points on vertical tiles and establishes this way a more closed, ITER like divertor magnetic configuration [12]. However, ASDEX Upgrade Div-I (in operation from 1991 to 1997) did establish a more open divertor geometry with both strike lines on the horizontal plates[10].

3. Experimental estimation of the SOL power flow

The SOL power flow profile is measured at the target and related back to the upstream profile using a simplified SOL model [6]). An exponential profile with decay length λ_q is assumed at the outer midplane separatrix region [15]. As power flows towards the divertor target, this is broadened by magnetic flux expansion, parameterised as f_x. Here, the definition for an integral flux expansion along the target surface [13,14] calculated for the outer midplane region $R = R_{sep}$ to $R = R_{sep} + 5$ mm, with R_{sep} being the outer separatrix radius, is used. The variation of f_x by using $R = R_{sep} + 2.5$ mm amounts to <5%.

By expressing the target coordinate as s and the strike line position on target as s_0 the heat load profile at the divertor entrance can be described as

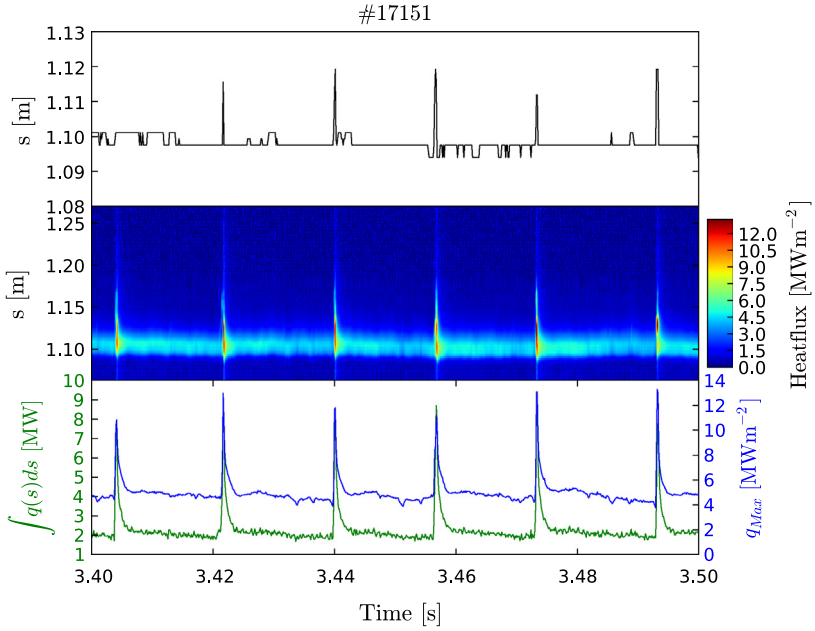

Fig. 2. Evolution of heat flux and the inferred strike line position on the divertor target for a typical ASDEX Upgrade discharge during type-I ELMy phase.

Table 1
Database of analysed discharges.

	#	I_p (MA)	B_T (T)	q_{95}	P_h (MW)	δ	Z_{eff}	f_{GW}
JET	60	1.0–3.5	1.1–3.2	2.6–5.5	5–24	0.2–0.4	1.5–2.5	0.44–0.88
AUG Div-IIb	22	0.8–1.0	1.5–2.4	3.2–5.1	2.5–12.5	0.2–0.4	2.0–2.7	0.46–0.74
AUG Div-I	4	1.0–1.2	1.9–2.0	2.6–3.0	5.0–7.5	≈0.1	≈2	≈0.5

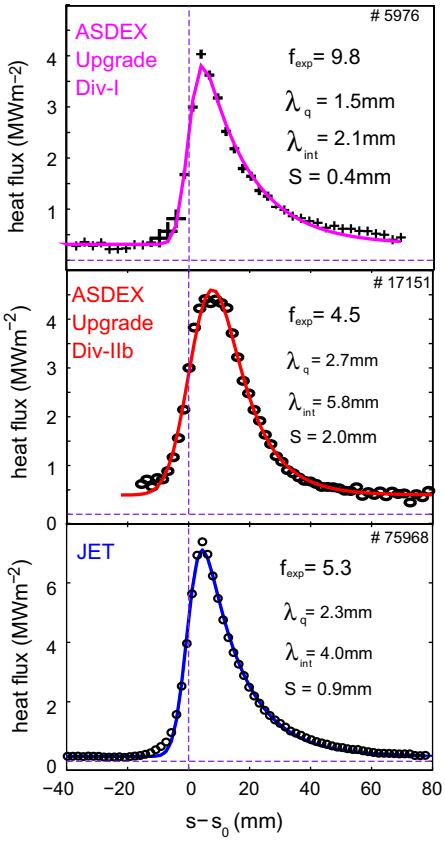

Fig. 3. Heat flux profiles measured on the outer divertor target and fits using Eq. (2) applied to heat flux data from JET and ASDEX Upgrade Div-I and Div-IIb.

$$q(\bar{s}) = q_0 \cdot \exp\left(-\frac{\bar{s}}{\lambda_q f_x}\right) \text{ and } \bar{s} = s - s_0, \quad s \geqslant s_0 \tag{1}$$

In addition to flux expansion, power flow in the divertor region is also assumed to be broadened by perpendicular heat diffusion which expands the profile deeper into the SOL and also into the private-flux-region (PFR) in a process known as *leakage* [16]. In this simple model, perpendicular diffusion is included by introducing a Gaussian, with a width S, which represents the competition between parallel and perpendicular heat transport in the divertor volume. This Gaussian is convoluted with the exponential profile [17]. The target heat flux profiles are thus expressed in a domain s element of $[-\infty, \infty]$.

$$q(\bar{s}) = \frac{q_0}{2} \exp\left(\left(\frac{S}{2\lambda_q}\right)^2 - \frac{\bar{s}}{\lambda_q f_x}\right) \cdot \operatorname{erfc}\left(\frac{S}{2\lambda_q} - \frac{\bar{s}}{S f_x}\right) + q_{BG} \tag{2}$$

Experimentally, heat flux profiles are measured on the outer divertor target by means of infrared thermography. Details of the experimental setup for JET can be found in Ref. [6] and for ASDEX Upgrade in Ref.[13]. These measurements are then related to the power decay length by fitting the parameters $S, \lambda_q, q_0, q_{BG}$ and s_0 in Eq. (2). Fig. 3 shows examples for measured heat flux profiles and their fits.

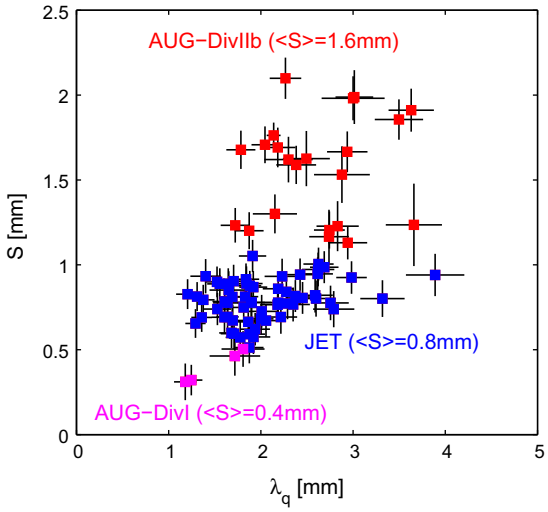

Fig. 4. Resulting values for λ_q and S from fitting for the complete database.

Fig. 4 shows the resulting values for λ_q and S from fitting for the complete database. Most notable here is that the values for S are largely varying when comparing JET, AUG Div-I and AUG Div-IIb and seem to cluster for each single divertor around a mean value. In particular it should be noted that for ASDEX Upgrade Div-I and Div-IIb largely different values for the power spreading parameter S are found. In contrast λ_q for both devices cover the same range from values of about 1 mm to 4 mm. Hence, in the JET machine, which has a radius of about 3 m, the shortest power fall-off widths are about 1 mm and are associated with the highest plasma currents. Also, values of about 1–4 mm are found for ASDEX Upgrade, a truly notable result.

4. Comparison of fit results to 2D-modelling of heat transport

The use of a Gaussian width (S) to describe the effects of the perpendicular cross-field and parallel along field diffusivities is a considerable simplification. However, this approximation has been validated by comparison with two-dimensional numerical heat diffusion calculations [18] using Spitzer-like ($\propto T^{5/2}$) parallel and Bohm-like perpendicular ($\propto T$) thermal diffusivities. The technique is found to be accurate to better than 15% in determining λ_q at the divertor entrance in cases where ratio of the deduced Gaussian width (S) and the exponential fall-off length (λ_q) is below unity as shown in Fig. 5. For the mean value of all JET data $S/\lambda_q = 0.4$ corresponding to 2% accuracy and for ASDEX Upgrade $S/\lambda_q = 0.57$ corresponding to 5% accuracy.

5. Approximate relation between λ_{int}, λ_q and S

The integral power decay width [14] at the divertor target can be derived from From Eq. (2) as

$$\lambda_{int} = \frac{\int (q(s) - q_{BG}) ds}{q_{max}} \cdot f_x^{-1} \tag{3}$$

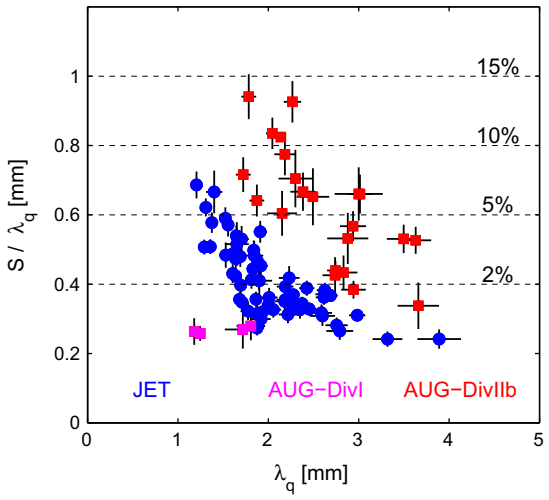

Fig. 5. The deviation of using a constant diffusion rather than solving the 2D numerical heat diffusion is dependent on S/λ_q and below 6% and 15% for JET and ASDEX Upgrade, respectively.

This quantity is frequently used in the literature [14] since it enables the peak heat load on the divertor target to be related to the power deposited on the divertor target, a crucial design parameter for the power handling capabilities of a large device such as ITER. It is shown by Makowski that, given the model for the target heat flux from Eq. (2) is applicable, the following relation is accurate to better than 3% for the analysed database[19]:

$$\lambda_{int} \simeq \lambda_q + 1.64 \cdot S \tag{4}$$

Fig. 6 shows a comparison between the experimental integral decay length λ_{int} (see Eq. (3)) and that calculated from Eq. (4) using the fitted λ_q and S. Good agreement is found. This suggests that, despite its simplicity, the fitting function stated in Eq. (2) well describes the experimentally measured heat load profiles. The most notable conclusion from Eq. (4) is that a regression of λ_{int} as a substitute for λ_q, as attempted in earlier studies [14], is unlikely to reveal the correct scaling parameters.

This becomes more evident upon closer examination of the typical values of λ_{int} for ASDEX Upgrade Div-I and ASDEX Upgrade Div-IIb and comparing them to λ_{int} values from JET. Regressing Div-I and JET data for λ_{int} would give positive major R dependencies, but regressing Div-IIb and JET data would give negative major R dependencies. As stated, this is in both cases an artefact from using λ_{int} rather than λ_q.

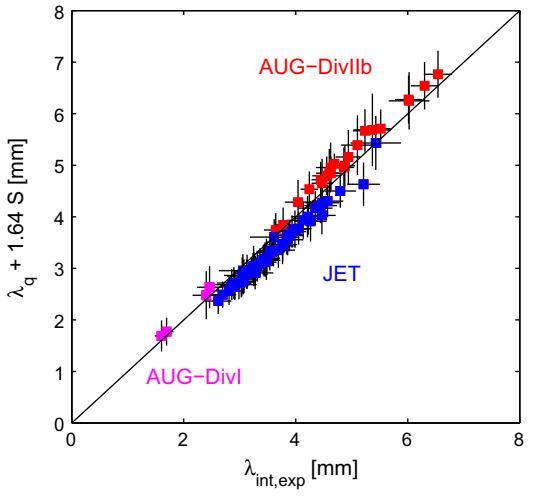

Fig. 6. Correlation between the experimental and fitted λ_{int} by using λ_q and S and applying the *Makowski relation* (Eq. (4)).

6. Multi parameter regression of λ_q

In this section, the empirical regressions of Ref. [9] are repeated on the extended database. In addition, a first regression using ASDEX Upgrade data only is performed and results from a combined scaling with DIII-D, C-Mod and NSTX are reviewed [19,20]. Taken together, these studies increase the confidence in the use of the empirical scaling.

For the new database, empirical regressions are provided for λ_q for JET and for the combined dataset from JET and ASDEX Upgrade deuterium discharges. The regression for ASDEX Upgrade is attempted despite the comparably poor variation in I_p and B_T. Hence, only a poor regression quality is found with large error bars for each regression variable. The regression parameters are B_T, cylindrical safety factor (q_{cyl}), power crossing the separatrix (P_{SOL}). In addition, R_{geo} is included when regressing combined data from JET and ASDEX Upgrade. Least square fitting is applied to derive a parametric dependency.

$$\lambda_q(\mathrm{mm}) = C_0 \cdot B_T^{C_B}(\mathrm{T}) \cdot q_{cyl}^{C_q} \cdot P_{SOL}^{C_P}(\mathrm{MW}) \cdot R^{C_R}(\mathrm{m}) \tag{5}$$

where,

$$q_{cyl} = \frac{2\pi a \cdot \epsilon \cdot B_T}{\mu_0 \cdot I_p} \cdot \frac{(1+\kappa^2)}{2} \tag{6}$$

Results are summarised in Table 2 for λ_q including the regression variances for each variable.

It can be seen that all the fits are consistent with each other within a single standard deviation. This suggests that similar physics is at work across all machines and illustrates the robustness of the empirical scaling. The fitted λ_q has a strong dependence on B_T and q_{cyl} and a minor dependency on P_{SOL}. Notably, no dependency of λ_q on R_{geo} is found. A comparison of the regressed versus the measured values are given in Fig. 7 for JET, ASDEX Upgrade Div-I and Div-IIb.

7. First results from 'tungsten' divertor operation in JET and ASDEX Upgrade

The analysis of Section 6 is performed solely on plasmas with carbon targets. However, due to its advantageous (i.e. lower) tritium retention, ITER and next step devices plan to use tungsten divertor targets. This has motivated experiments in JET and ASDEX Upgrade to test the applicability of the scalings of Section 6 for plasmas with tungsten divertors. Experiments have been performed in JET with the JET-ILW tungsten divertor [21] with dedicated scans in plasma current (1–2.8 MA) and toroidal field (1–2.5 T). Low density ASDEX Upgrade discharges have been per-

Table 2
Parameter dependency of λ_q using Eq. (5).

			C_0	C_B	C_q	C_P	C_R	R^2
JET	λ_q		0.70	−0.85	1.23	0.13	–	0.68
		±	0.23	0.26	0.24	0.12	–	
AUG	λ_q		0.78	−0.63	1.14	−0.05	–	0.43
		±	0.69	1.05	0.81	0.31	–	
JET + AUG	λ_q		0.90	−0.73	1.16	0.04	−0.11	0.61
		±	0.37	0.26	0.27	0.12	0.15	
D3D + NSTX + CMod	λ_q		0.93	−0.97	1.09	−0.10	–	0.79
		±	0.26	0.06	0.20	0.09	–	

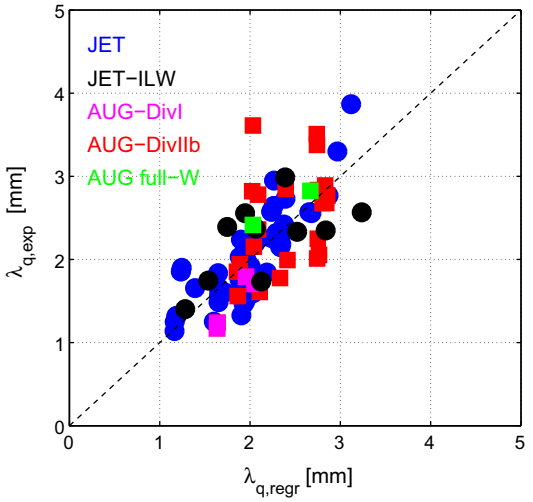

Fig. 7. Comparison of predicted (see JET + AUG fit in Table 2) versus measured values for λ_q.

formed at 1.2 MA, 2.5 T, 12.5 MW NBI and 3 MW ECRH heating with the full tungsten wall [22]. Note that the divertor geometry of full-W ASDEX Upgrade operation is nearly identical to ASDEX Upgrade Div-IIb. Identicals diagnosis and analysis method to that presented for the plasmas with carbon divertors was used for these plasmas.

As can be seen from Fig. 7, both the JET and ASDEX Upgrade tungsten divertor plasmas have SOL power decay widths which are consistent with the multi parameter regression to the combined JET and ASDEX Upgrade database of Section 6. Thus, these expressions can be applied with some confidence to plasmas with both carbon and tungsten divertors.

8. Comparison between the power fall-off in L-mode and H-mode plasmas

The presented studies were recently extended for dedicated L-mode discharges or short L-mode phases before transition to H-mode for both, JET and ASDEX Upgrade. A detailed discussion can be found in [23]. For all cases it is found that $\lambda_{q,\mathrm{L-mode}} > \lambda_{\mathrm{SOL,H-mode}}$. For most cases $\lambda_{q,\mathrm{L-mode}}$ is 2–3 times larger than predicted by the H-mode scaling. This is expected, as radial transport in L-mode plasma is larger than in H-mode equivalents in the edge plasma. Slightly different results are achieved for the L-mode regression of λ_q depending on the chosen database from JET and ASDEX Upgrade as no dedicated scans for L-mode plasmas, in contrast to the H-mode studies, are available. The best results w.r.t. best regression residuals from least square fitting for a combined JET and ASDEX Upgrade database are:

$$\lambda_q^{\mathrm{L-mode}}(\mathrm{mm}) = 1.37 \cdot B_T^{-0.55}(\mathrm{T}) \cdot q_{cyl}^{1.17} \cdot P_{\mathrm{SOL}}^{0.2}(\mathrm{MW}) \cdot R^{0.1}(\mathrm{m}) \qquad (7)$$

Most worth notifying here is that the L-mode regression parameter are reminiscent of those found for H-mode plasmas but with an approximately 2 times larger constant, hence larger values for λ_q in L-mode. When extrapolating to ITER for L-mode plasma by using Eq. (7) and $P_{\mathrm{SOL}}^{\mathrm{L-mode}} = 50$ MW a value for λ_q of 3.8 mm is found for ITER. Following the studies in [23] $\lambda_q^{\mathrm{L-mode}}$ is between 3.4 mm and 5.5 mm.

9. Conclusions

A simplified model for power flow in the SOL has enabled the independent estimation of the integral divertor target (λ_{int}) and exponential SOL (λ_q) power fall-off widths and an effective power spreading parameter (S). The most notable conclusion of the analysis of λ_q is that no machine size scaling is detected. The design values for the ITER baseline are $R = 6.2$ m, $a = 2.0$ m, $\kappa = 1.7$, $P_{\mathrm{SOL}} = 120$ MW, $B_{tor} = 5.3$ T, $I_p = 15$ MA, $q_{cyl} = 2.42$, $Z_{eff} = 1.6$ [32]. Extrapolation of the regression analysis from Table 2 results in $\lambda_q^{ITER} \simeq 1$ mm.

Recent experiments carried out with 'tungsten' divertors in JET and ASDEX Upgrade revealed no deviations from the results with carbon plasma-facing-components. Also the comparison λ_q to the prediction of the heuristic drift based model [24], based on parallel convection and curvature drifts, is satisfactory with regard to both magnitude and scaling and newer results from 'tungsten' divertor confirm the latter statement.

However, extrapolation of λ_{int} to ITER cannot be performed from this work. Such an extrapolation requires a reliable regression of S from the current database which is not yet achieved. Such an attempt has to include an understanding of the effect of the divertor geometry on the power spreading S parameter. Also accompanying code simulations seem to be necessary focussing on discharge conditions in absence of detachment processes [25–27].

However, the huge observed difference of the S parameter between ASDEX Upgrade Divertor-I and Divertor-IIb gives hope that a sufficiently large S in the long baffled ITER divertor will be present and hence will cause $\lambda_{int} \gg \lambda_q$. As an exercise, purely for curiosity, the S value from ASDEX Upgrade Div-IIb can be assumed for ITER, in which case λ_{int} can be calculated as

$$\lambda_{int}^{ITER}(\mathrm{mm}) = 1\ \mathrm{mm} + 1.64 \times 1.6\ \mathrm{mm} = 3.6\ \mathrm{mm} \gg 1\ \mathrm{mm} \qquad (8)$$

It is noted that if S is large enough, radial diffusion dominates and the actual value of λ_q would be of minor importance for the resulting λ_{int} value. Only dedicated experiments aiming to find a scaling of S, can lead to a better understanding here, e.g. by varying the distance between x-point and divertor target plate in controlled experiments with otherwise fixed discharge parameters (i.e. constant λ_q) as executed in DIII-D [28] recently.

ITER is anticipated to operate in conditions with a high fraction of SOL radiation and partially detached divertor plasmas, unlike the conditions studied here. However, the assumption [29] that λ_q will be in the range of 5 mm needs to be compared to consequences for operation and divertor detachment accessibility arising from the prospected result of $\lambda_q \approx 1$ mm, as aimed for in [30]. Finally, it should be noted that the results here from simple regression analysis are not constrained by other effects which may be present and would be violated by a power fall-off length of 1 mm in the outer midplane in ITER [31].

Acknowledgements

The authors want to thank O. Kardaun, T. Pütterich and C. Lowry for support and discussions. In particular we thank A.W. Leonard and M. Makowski from DIII-D and J. Terry from Alcator C-Mod for highly valuable discussion. Further credit is paid to the support of the IR team in JET, i.e. S. Devaux, G. Arnoux and I. Balboa and P. de Marne from ASDEX Upgrade. This work was supported by EURATOM and carried out within the framework of the European Fusion Development Agreement. The views and opinions expressed herein do not necessarily reflect those of the European Commission.

References

[1] F. Wagner et al., Phys. Rev. Lett. 49 (1982) 1408.
[2] D. Hill et al., J. Nucl. Mater. 241–243 (1997) 182.
[3] T. Eich, A. Herrmann, J. Neuhauser, Phys. Rev. Lett. 91 (2003) 195003.
[4] S. Devaux et al., J. Nucl. Mater. 415 (2011) S865.

[5] A. Wingen, T.E. Evans, C.J. Lasnier, K.H. Spatschek, Phys. Rev. Lett. 104 (2010) 175001.
[6] T. Eich et al., J. Nucl. Mater. 415 (2011) S856.
[7] E. Solano et al., Nucl. Fusion 48 (2008) 065005.
[8] M.G. Dunne et al., Nuclear Fusion 52, 123014 (2012).
[9] T. Eich et al., Phys. Rev. Lett. 107 (2011) 215001.
[10] A. Herrmann et al., Fusion Sci. Technol. 44 (2003) 569.
[11] S. Brezinsek et al., J. Nucl. Mater. 415 (2011) S936.
[12] A. Kallenbach et al., J. Nucl. Mater. 415 (2011) S19.
[13] A. Herrmann et al., Plas. Phys. Contr. Fus. 44 (2002) 883.
[14] A. Loarte et al., J. Nucl. Mater. 266–269 (1999) 587.
[15] P. Stangeby et al., Nucl. Fusion 50 (2010) 125003.
[16] A. Loarte et al., Contrib. Plasma Phys. 32 (1992) 468.
[17] F. Wagner, Nucl. Fusion 25 (1985) 525.
[18] R. Goldston, Phys. Plasmas 17 (2010) 012503.
[19] M.A. Makowski et al., Physics of Plasmas 19 (2012) 056122 (9 pp.).
[20] R.Maingi et al., these proceedings.
[21] G. Matthews et al., these proceedings.
[22] R. Neu et al., these proceedings.
[23] A. Scarabosio et al., these proceedings.
[24] R. Goldston, Nucl. Fusion 52 (2012) 013009.
[25] M. Wischmeier et al., J. Nucl. Mater. 415 (2011) S523.
[26] B. Lipschultz et al., J. Nucl. Mater. 241–243 (1997) 771.
[27] M. Fenstermacher et al., Plas. Phys. Con. Fusion 41 (1999) A345.
[28] T.W. Petrie et al., these proceedings.
[29] ITER Phys. Exp. Group, Nucl. Fusion 47, S203 (2007).
[30] A. Kukushkin et al., these proceedings.
[31] D. Whyte et al., these proceedings.
[32] B.J. Green et al., Plas. Phys. Con. Fusion 45 (2003) 687.